JOURNAL OF MATERIALS SCIENCE 29 (1994) 6019–6025

Microstructural analysis of Fe–Si–Al alloy powders and films by Mössbauer spectrometry

K. NOMURA
Faculty of Engineering, University of Tokyo, Hongo 7-3-1, Bunkyo-ku, Tokyo 113, Japan
Y. UJIHIRA
Research Center of Advanced Science and Technology, University of Tokyo, Komaba 4-6-1, Meguro-ku, Tokyo 153, Japan
A. YANAGITANI
Sanyo Special Steel Co., Ltd. Nakashima 3007, Shikama-ku, Himeji, 672, Japan
N. KAWASHIMA
Tokyo Magnetic Printing Co. Ltd, Onodai 2-29-20, Sagamihara City, Kanagawa, 229, Japan

The powder, plate and films of Fe–Si–Al alloy were prepared by gas atomizer, extrusion, sputtering, and quenching. The characteristics of these alloy materials were studied by Mössbauer spectrometry, and estimated on the base of iron configuration. The magnetic hyperfine fields were dependent on each preparation process. Quenched ribbon gave a perfect DO_3 structure.

1. Introduction

The ternary alloy of iron–silicon–aluminium with the composition 9.62 wt % Si, 5.38 wt % Al and Fe balance, i.e. sendust alloy, shows excellent soft magnetic characteristics (internal permeability 117 500, magnetic hysteresis loss 2.8 J m^{-3} per cycle) [1]. Fe–Si–Al alloy can form continuous substitutional solid solutions. Aluminium and silicon atoms develop during ordering from a B2 structure (paramagnetic) to a DO_3 structure (ferromagnetic). The α structure transforms to DO_3 at 650° C [2]. Cast Fe–Si–Al alloy has poor workability from the industrial point of views. Conventionally it must first be pulverized from an ingot form for the industrial application. The properties of sendust powders change depending on preparation methods. During the powdering process of ball milling, the crystalline structure of the alloy powders was affected by mechanical force [3]. Phase separation in the ordered alloy is caused by the contribution of excess free energies due to ordering [4]. The effect of particle size and particle shapes was studied by conversion electron Mössbauer spectrometry (CEMS) [5], which is an effective method of microstructure analysis of surface layers of particles, as well as films.

Gas atomization is one method suitable for producing homogeneous powders, and large-scale materials can be produced by consolidation and extrusion of gas-atomized powders. Target materials for sputtered films can be prepared by this method. The target discs are found to be composed of more uniform grains of about 100 μm and to have a higher density of 6.96 $\times 10^3$ kg m^{-3} than as-cast alloy (6.91 $\times 10^3$ kg m^{-3}) [6].

In the present work, the sendust alloy of gas-atomized powders, disc targets and sputtered films were characterized by conventional transmission and conversion electron Mössbauer spectrometry; quenched alloy and cast alloy were also analysed for comparison.

2. Experimental procedure

Fe–Si–Al master alloy was prepared in a vacuum induction furnace. Fe–9.6%Si–5.4%Al ($Fe_{73.7}$ $Si_{16.6}$ $Al_{9.7}$) powder was produced directly from the master alloy in a gas atomizer using argon gas at a pressure of 6 atm. The average diameters of sphere powders were 70–100 μm. Powders with diameters less than 40 μm were sieved, and Mössbauer spectra were measured. A steel capsule filled with the powder was evacuated, sealed by welding and hot pressed at 1473 K and about 60 kg mm^{-2} in an extrusion press. The encapsulated material was slowly cooled in sand to avoid cracking after the consolidation and its steel capsule was removed [6]. The sendust films on silicon wafers were prepared from the target disc by the argon sputtering method. The sputtering apparatus and conditions were as follows: Nichiden Anelba: SPF-332H, argon pressure 2.4–2.0 Pa, distance between the electrode and sample 80 mm, rotation of the cooled substrate 10 r.p.m., d.c. sputtering power 500 W.

The composition of sputtered film was determined to be 85.44% Fe–9.68% Si–4.88% Al ($Fe_{74.4}$ $Si_{16.8}$ $Al_{8.8}$), which was lower in aluminium content than the target material. A quenched sample was also prepared by a rolling method (3000 r.p.m., 30 cm diameter copper single roll) to enable comparison with gas-atomized powders and extruded alloy. Conventional

0022–2461

transmission Mössbauer spectra (TMS) were measured with 370 MBq ^{57}Co(Rh) at room temperature, using a scintillation counter as a detector. Conversion electron and X-ray Mössbauer (CEM and XM) spectra were obtained with a proportional counter [7], flowing He + 5% CH_4 and Ar + 5% CH_4, respectively. The incident γ-rays were irradiated perpendicular to the surface of the films. Data were analysed by a several Lorenzian peaks. X-ray diffraction and electron probe microanalysis were used, respectively, to confirm the structure and the distribution of aluminium, silicon and iron on grains.

3. Results and discussion

Typical X-ray diffraction patterns of the gas-atomized powder, hot-extruded sample, quenched sample, sputtered film and its annealed film at 400 °C for 2 h are shown in Fig. 1. Because the (1 1 1) and (3 1 1) lines were observed in X-ray diffraction patterns of the gas-atomized sample, hot-extruded sample and quenched sample, these alloys had a DO_3-type superlattice. The peaks corresponding to superlattice diffraction could not be observed in sputtered samples or (2 2 0) and (2 2 2) peaks indicative of body centred cubic structure (b c c).

Three crystal structures are known for sendust alloy, as shown in Fig. 2 [8]; the ordered structure of B2, DO_3 and the disordered structure of α-type. The atomic configurations of B2 and DO_3 ordered structures in b c c ternary alloy are as follows. The unit cell of DO_3 superlattice is divided into four f c c sublattices as shown in Fig. 2. The atoms in sublattices A and C are the nearest neighbour (nn) to the atoms in sublattices B and D. The atoms in sublattice A or B are the next nearest neighbours (nnn) to the atoms in C or D, respectively. At a concentration of 25 at % Si + Al, the A, C, D sites are occupied by iron atoms, and the B site is occupied by silicon or aluminium atoms. When silicon or aluminium at the B site and iron at the D site are mixed randomly, ($r_A \neq r_B$ and $r_A = r_C$, $r_B = r_D$), it becomes a B2 ordered lattice. When iron, aluminium and silicon occupy with the same probabilities, a b c c disordered lattice results. In DO_3 structure, one-third of the iron atoms occupy the sites surrounded by eight iron atoms, and two-thirds of the iron atoms occupy the sites surrounded by 4Fe and 4(Si, Al) atoms.

On the basis of the above facts, powders and films of sendust alloy were analysed by computer fitting and the results of Mössbauer parameters are summarized in Table I.

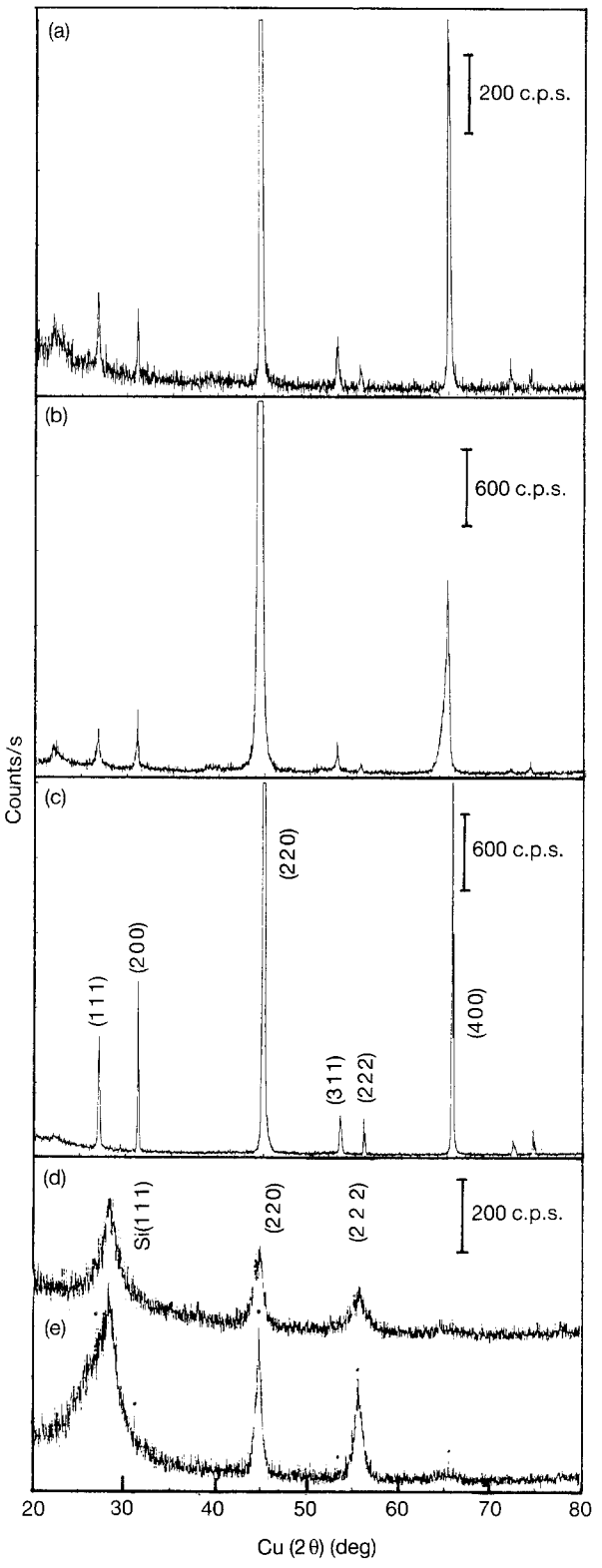

Figure 1 X-ray diffraction patterns of (a) gas-atomized powder, (b) extruded sendust plate pressed from gas-atomized powder, (c) quenched sendust ribbon, (d) as-sputtered films, and (e) the sputtered film annealed at 400° C for 2 h.

3.1. Gas-atomized powders

The Mössbauer spectrum of gas-atomized powders is shown in Fig. 3. The spectrum was decomposed into four magnetic components, of which the hyperfine fields were 29.7, 27.4, 20.2, and 19.8 T, respectively. Because the component of 27.4 T was included, the atomized powder did not always have a perfect DO_3 structure, it was termed the DO_3-like structure. The full-width at half maximum (FWHM) of these outer peaks were broad (0.527 mm s^{-1}), indicating that iron sites fluctuated slightly, i.e. in a somewhat disordered state. The magnetic fields of 29.7 and 27.4 T were assigned to iron sites, surrounded by 8Fe0(Si, Al) in the nearest neighbour and further affected by silicon or aluminium atoms in the next nearest neighbours, respectively. The magnetic fields of both 20.2 and 19.8

TABLE I Mössbauer parameters of Fe–Al–Si alloy prepared by many methods

Sample	Site[a]	H_{in} (T)	IS (mm s^{-1})	QS (mm s^{-1})	Intensity (%)
Gas-atomized powder, TMS	Fe1	29.7	0.07	0.02	27.7
	Fe5	27.4	0.06	0.07	7.8
	Fe2	20.2	0.16	− 0.04	31.3
	Fe3	19.8	0.32	0.06	33.2
Extrusion alloy, CEMS	Fe1	29.2	0.04	− 0.01	9.6
	Fe4	25.4	0.10	0.01	20.6
	Fe2	21.4	0.14	− 0.02	25.0
	Fe6	16.8	0.28	0.0	18.3
	Fe7	12.3	0.17	− 0.16	26.5
Extrusion alloy annealed	Fe1	28.4	0.08	0.02	28.6
at 850 °C for 1 h, CEMS	Fe4	24.7	0.14	0.01	27.6
	Fe2	20.4	0.23	− 0.02	23.0
	Fe6	17.6	0.35	0.19	9.0
	Fe7	13.2	0.29	− 0.31	11.7
Sputtered film as-deposited, CEMS	Fe1	30.2	0.09	− 0.21	35.8
	Fe5	27.2	0.01	0.27	29.2
	Fe4	23.7	0.19	− 0.24	23.7
	Fe3	19.5	0.25	0.01	1.5
	D1	–	0.29	− 0.82	5.3
	D2	–	0.11	− 1.37	7.9
Sputtered film annealed at 400 °C	Fe1	32.2	0.06	− 0.06	36.8
for 2 h. CEMS	Fe5	29.0	0.05	0.06	27.4
	Fe4	24.9	0.15	− 0.04	19.3
	Fe2	20.3	0.19	0.11	12.1
	D1	–	0.29	− 0.95	1.6
	D2	–	0.05	− 1.49	2.7
Quenched ribbon, CEMS	Fe1	29.4	0.08	0.01	39.2
	Fe2	20.4	0.13	− 0.08	25.3
	Fe3	20.0	0.34	0.07	35.5
Quenched ribbon, TMS	Fe1	29.2	0.07	− 0.01	37.7
	Fe2	20.1	0.19	− 0.04	32.3
	Fe3	19.7	0.33	0.09	30.0
Cast (flake-type powder) annealed at	Fe1	32.3	0.04	− 0.01	32.5
800° C for 3 h	Fe5	28.9	0.06	0.03	21.1
	Fe4	24.7	0.19	0.01	24.6
	Fe2	19.6	0.23	− 0.05	21.8
Cast (granular-type powder annealed at	Fe1	30.8	0.06	0.01	38.0
800° C for 3 h	Fe4	25.1	0.18	0.02	6.8
	Fe2	20.6	0.17	− 0.07	31.8
	Fe3	20.2	0.34	0.08	23.4
Cast ingot XMS	Fe1	29.7	0.09	0.01	23.8
	Fe4	26.2	0.12	− 0.10	10.0
	Fe2	20.4	0.16	− 0.01	21.9
	Fe3	19.7	0.35	0.11	28.7
	Fe7	11.7	0.33	0.07	15.7

[a] Site of iron environments:
Fe1 = 8Fe0(Si, Al), Fe2 = Al poor 4Fe4(Si, Al),
Fe3 = Si-poor 4Fe4(Si, Al), Fe4 = 6Fe2(Si, Al),
Fe5 = 8' Fe0(Si, Al), Fe6 = deformed 4Fe4(Si, Al),
Fe7 = deformed 3Fe5(Si, Al).
D1 = superparamagnetism of Fe2 and Fe3,
D2 = superparamagnetism of Fe1 and Fe5.

T were due to iron atoms surrounded by 4Fe and 4(Si, Al) atoms with different contents of silicon and aluminium.

The spectrum of cast Fe–Si–Al alloy is shown in Fig. 4. The components of 26.2 and 11.7 T were included in cast alloy in addition to the magnetic fields of 29.7, 20.4 and 19.7 T in the ordinary DO_3 structure, for which the intensity ratio was approximately 24:22:28. The magnetic field of 26.2 and 11.7 T might be assigned to the iron environments of 6Fe2(Si, Al) and distorted 3Fe5(Si, Al). These results indicate that gas-atomized powders produced a better microstructure in sendust alloy than in cast iron. This was considered to be caused by the deviation of the composition from the stoichiometry of DO_3 structure in micrograins because cast iron had the large elemental deviation of silicon and aluminium. Transmission and X-ray Mössbauer spectra of gas-atomized powders and cast alloy gave the bulk information. In both spectra, the peak intensity ratio was $I_{1.6}:I_{2.5}:I_{3.4} \simeq 3:3:1$, where $I_{i,j}$ stands for the intensity of the ith and jth sextet peaks from the left. The directions of magnetic fields were nearly at random in the bulk of several tens of micrometres thickness.

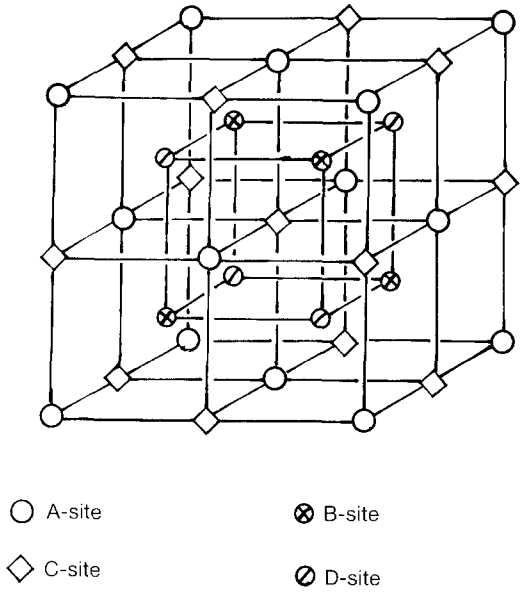

Figure 2 Unit structure of Fe–Si–Al sendust alloy.

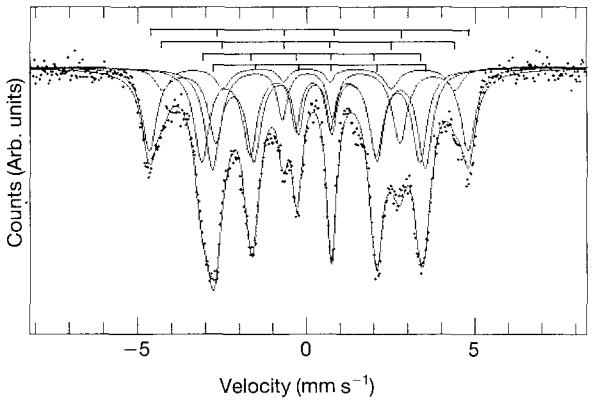

Figure 3 Transmission Mössbauer spectrum of gas-atomized powders.

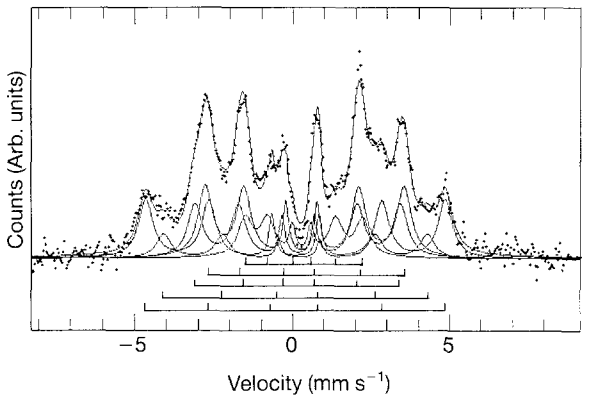

Figure 4 X-ray Mössbauer spectrum of cast sendust ingot.

3.2. Extruded plate

The Mössbauer spectra of the sendust disc prepared by the extrusion of gas-atomized powders and its annealed disc are shown in Fig. 5. After consolidation and extrusion of the gas-atomized powders, the intensity of the magnetic field of 29 T decreased and the magnetic field of 25 T appeared, whereas the intensi-

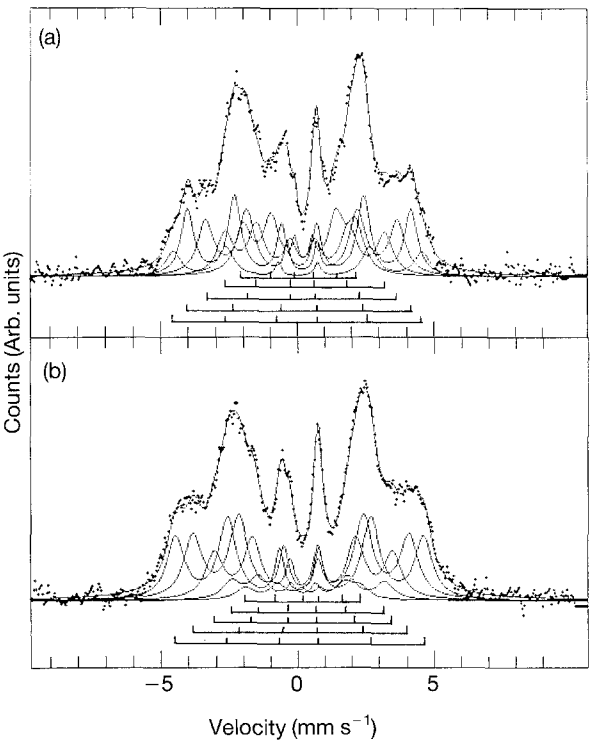

Figure 5 Conversion electron Mössbauer spectra of extruded disc prepared from gas-atomized powders and its annealed disc of sendust alloy.

ties of small hyperfine fields were relatively high and a large electric field gradient around magnetic iron sites was observed. X-ray diffraction patterns with the small broadened peaks suggested that the whole structure could also be distorted. The (400) plane, in particular, was slightly distorted by the extrusion. The Mössbauer spectra gave clearer information on the serious change in microstructure. Although each spectrum was deconvoluted into five sextets by refitting many times, each sextet was hard to reduce in a specified iron site because they were distorted from a perfect DO_3 structure. However, Mössbauer spectra showed that the DO_3-like structure was transformed to the more distorted state by extrusion. When the extruded sample was annealed at 850 °C for 1 h, the intensity of a largest hyperfine field increased. However, the distortion could not be perfectly released in the ordered state of DO_3, because a small magnetic field with the electric field gradient remained. The direction of magnetic spins in a layer about 100 nm thick on the extruded plate was parallel to the surface, because each peak ratio of five sextets was close to $I_{1.6}: I_{2.5}: I_{3.4} = 3:4:1$.

In the extruded sendust prepared from gas-atomized powders, the deviation of elements was small and the distribution of elements was homogeneous, as compared with cast alloy, and also the density was 6.96 g cm^{-3}, which was higher than that of conventional cast alloy (6.912 g cm^{-3}) [6]. The target disc with a uniform fine-grain size of about 100 μm and without segregation, is machinable. However, the hyperfine fields were smaller than those of DO_3 structure. Stearns [9] reported that annealed binary iron silicon alloy with 14–27 at % Si showed peaks at 28.7,

24.3 and 14.5 T, which were attributed to internal magnetism due to the iron environments of 6Fe2Si, 5Fe3Si, and 3Fe5Si, respectively. Arita *et al.* [8] proposed that the effect of next nearest neighbouring atoms should be also taken into account, and that binary sendust of Fe–Si alloy consists of five components of 3Fe5Si, 4Fe4Si, 5Fe3Si, 6Fe2Si, and 8Fe0Si in the nearest neighbour sites. The relation between the hyperfine field, (H_{in}, and the number of silicons in the nearest neighbour and in the next nearest neighbour around the iron atom is expressed as follows.

$$H_{in} = 32.1 - 1.184(\text{nn Si})^{1.668} - 0.14\cdot(\text{nnn Si}) \quad (1)$$

A similar analysis was reported for binary Fe–Al ordered alloys [10]. Assuming that aluminium can substitute a part of silicon, the relation can be applicable to the ternary alloy. The small hyperfine fields of about 17 and 13T might be attributed to distorted iron environments of 4Fe4(Si, Al) and 3Fe5(Si, Al) respectively.

3.3. Sputtered films

Fig. 6 shows the Mössbauer spectra of the sputtered film and its annealed film, prepared from the extruded disc. Two doublets were observed in addition to the sextets. These paramagnetic peaks were considered to be due to the superparamagnetism of fine crystalline grains. From the peak width of the X-ray diffraction pattern, the crystalline size was calculated to be about 11 nm. The (2 2 0) plane was oriented on the Si (1 1 1) plane substrate, of which broad diffraction peaks appeared at about $2\Theta = 28°$. The doublet with a small electric field gradient was attributed to iron environments having many silicon and aluminium atoms such as 4Fe4(Si, Al), and the other with a large electric field

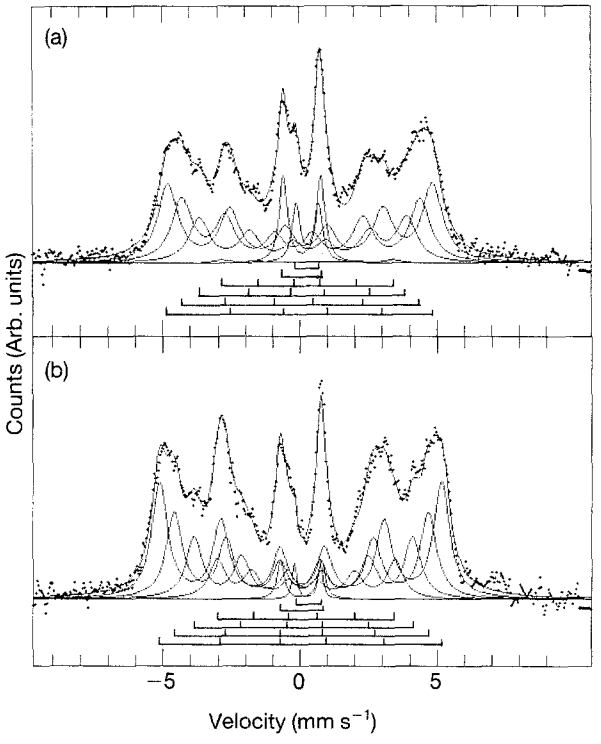

Figure 6 Conversion electron Mössbauer spectra of d.c. sputtered film and its annealed film at 400° C for 2 h.

to silicon- and aluminium-poor iron environments such as 8FeO(Si, Al). The intensity of these doublets were decreased and the corresponding sextets were increased by annealing at 400° C for 2 h. The direction of the magnetic spins in the surface about 100 nm thick, was at random, because the sextets had the intensity ratio $I_{1.6}$: $I_{2.5}$: $I_{3.4} = 3:2:1$. Fine grains contained in the d.c. sputtered films were considered to contribute to the decrease in anisotropic magnetism, that is, random orientation. These tendencies were different from r.f. sputtered films analysed by Miyazaki *et al.* [11]. The spin directions in sputtered Fe–Al–Si thin films on crystallized-glass substrate, prepared by an r.f. planar magnetron sputtering, are parallel to the surface. Using r.f. magnetron sputtered films, the correlation between the structural change and the soft magnetic properties was clarified. Low coercive force, high effective permeability, and low electrical resistivity were obtained for the r.f. sputtered films annealed at 500° C, which showed DO_3 ordered structure. The probability of the distribution aluminium and silicon atoms in the 4Fe4(Si, Al) environment was estimated as follows [11]: 15% for (4Si, 0Al) distribution, 36% for (3Si, 1Al), 33% for (2Si, 2Al), 14% for (1Si, 3Al) and 2% for (0Si, 4Al). The thermal stability of the DO_3 structure in the sendust film was different from the bulk because aluminium was easily segregated on the surface. In d.c. sputtered films, the hyperfine distributions and each intensity were different from those of an ideal DO_3 ordered structure. A study of the d.c. sputtered sendust films annealed at various temperatures was reported by Nomura *et al.* [12].

3.4 Quenched ribbons

Attempts were made to produce a sendust ribbon by the quenching method using a single rolling cooler; excellent sendust with an ideal DO_3 structure was obtained, as shown in Fig. 7. The Mössbauer spectra were composed of three iron environments surrounded by 8Fe and 4Fe4(Si, Al). The latter can be decomposed into two iron environments; one is aluminium-poor 4Fe4(Si, Al) such as 4Fe(4Si, 0Al) and 4Fe(3Si, 1Al), and the other silicon-poor 4Fe4(Si, Al) such as 4Fe(2Si, 2Al) and 4Fe(1Si, 3Al), because Dobrzynski *et al.* [13] reported that isomer shift increased slightly with the increase in aluminium content. Ono *et al.* [14] reported that the isomer shift for the iron site surrounded by 4Fe4Al atoms was 0.28 mm s^{-1}. Frankowiak [15] reported that the internal magnetic field and isomer shift in Fe_3Al alloy were dependent on the degree of ordering. The sextet of the hyperfine field of about 20 T with a small isomer shift corresponds to iron environments of 4Fe(4Si, 0Al) and 4Fe(3Si, 1Al), and the sextet of about 20 T with a large isomer shift corresponds to that of 4Fe(2Si, 2Al) and 4Fe(1Si, 3Al). From the CEM and TM spectra, it was found that the surface of quenched sendust was slightly different from the bulk, because of the different intensity ratio of aluminium-poor 4Fe4(Si, Al) to silicon-poor 4Fe4(Si, Al). The bulk was an ideal DO_3 structure, but a change in aluminium or silicon in the surface might affect the iron environments of

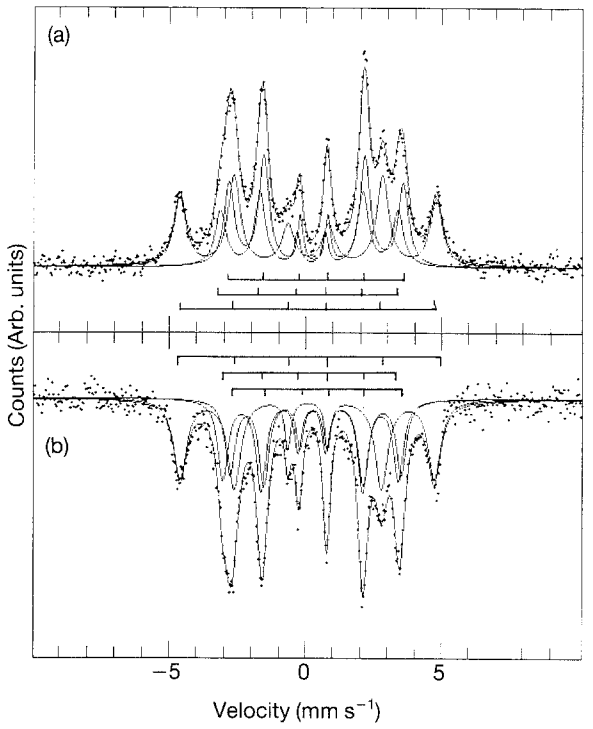

Figure 7 (a) Conversion electron Mössbauer spectrum and (b) transmission Mössbauer spectrum, of quenched sendust prepared by a single-roll method.

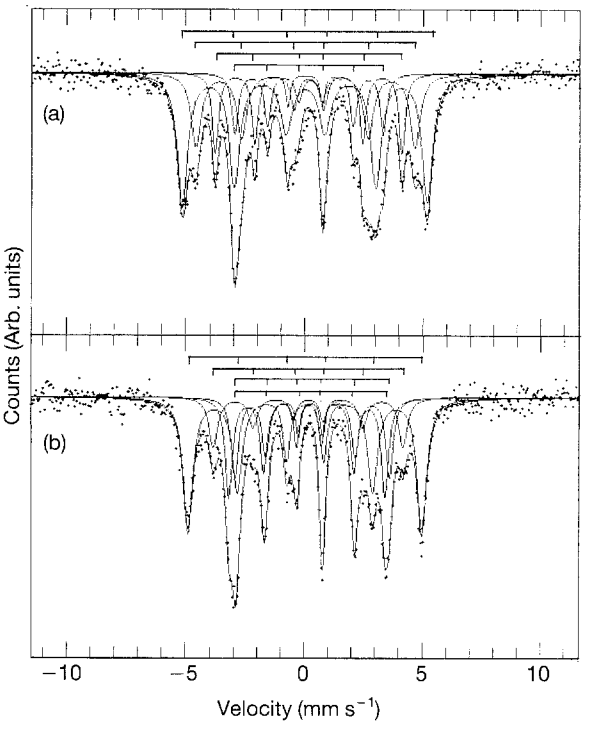

Figure 8 Mössbauer spectra of (a) flake- and (b) granular-type sendust powders, less than 25 μm in size, heated at 800° C for 3 h.

4Fe4(Si, Al), although these hyperfine fields did not vary so much. The peak width of X-ray diffraction peaks of the quenched sample was narrow. The full width at half maximum (FWHM) of the (2 2 0) peak due to the quenched sample was 0.08°, whereas the FWHM of gas-atomized powders and hot-extruded plates were 0.24° and 0.44°, respectively.

3.5 Powders prepared from cast alloy

When cast iron was pulverized mechanically by ball milling, the microstructure was largely affected, and the magnetic fields were different between the formation of flake- and granular-shaped powders. Two prevalent peaks of 13 and 24 T and three peaks of 12, 19 and 25 T were observed in magnetic hyperfine distributions of flake- and granular-shaped powders, respectively. No magnetic field of 29.7 T was observed in either sample [5]. The defects and distorted microstructure produced caused the hyperfine fields to decrease greatly. In order to confirm the reformation of deformed hyperfine structures, flake- and granular-shaped powders were annealed at 800° C for 3 h in a 5% H_2 + 95% N_2 atmosphere. It is known that DO_3 structure in the bulk sendust is stable up to 850° C. The deformed DO_3 structure should be released by annealing. However, different Mössbauer spectra were obtained between flake- and granular-type powders annealed as shown in Fig. 8. The latter was close to a DO_3-like structure with the iron environments of 8Fe0(Si, Al) and 4Fe4(Si, Al), although the component corresponding to the iron environment (25 T) of 5Fe3(Si, Al) was included slightly. The magnetic fields of 32.3, 28.9, 24.7 and 19.6 T were observed in the flake-type powders annealed, and the peak intensities were very different from those of the DO_3 ordered structure. Each magnetic field corresponded to iron environments of 8Fe0(Si, Al), 6Fe2(Si, Al), 5Fe3 (Si, Al), and 4Fe4(Si, Al). These results suggested that in flake-type powders, the large segregation of silicon or aluminium occurred with the deformation of DO_3 structure by the powdering process.

4. Conclusion

Powders and films of Fe–Si–Al ternary alloy were prepared by gas-atomization, extrusion, sputtering, and quenching methods. The results are summarized as follows. The powders and films had specified hyperfine fields, which were affected by defects of the crystal structure and the local distribution of silicon and aluminium atoms around iron atoms. The structure of gas-atomized powders was near to the DO_3 structure. However, hot pressing and extrusion largely distorted the structure. Once the powders had deviated from an ideal composition in the DO_3 microstructure, the latter could not be easily recovered by annealing. In the sputtered films, fine grains were included which led to the random orientation of magnetic spins. Sendust ribbon with near-perfect DO_3 structure was obtained by a quenching method. This is expected to show more excellent and attractive magnetic properties as a soft magnetic material. CEMS can be effectively applied to the analysis of the surface layers on powder grains and films of sendust alloy. The analysis of changes in the hyperfine fields is a sophisticated method for differentiating the quality of sendust alloy.

References

1. H. MASUMOTO and T. YAMAMOTO, *Jpn Inst. Metals* **1** (1937) 127.

2. Y. CHANG, *Acta Metall.* **30** (1982) 1185.
3. K. NOMURA, Y. UJIHIRA, M. SUEKI and N. KAWASHIMA, *Hyperf. Inter.* **54** (1990) 839.
4. M. FUKAYA, T. MIYAZAKI and T. KOZAKI, *J. Mater. Sci.* **26** (1991) 5420.
5. K. NOMURA, Y. UJIHIRA and N. KAWASHIMA, *Nucl. Instr. Methods in Phys. Res.* **76** (1993) 199.
6. A. YANAGITANI and Y. TANAKA, in "Proceedings of The Second Japan International SAMPE Symposium and Exhibition", edited by I. Kimpara, K. Kageyama, Y. Kagawa, Chiba, 11–14 December, 1991, (Soc. for the Advancement of Material and Process Engineering, Tokyo, 1991) pp. 1019–26.
7. K. NOMURA and Y. UJIHIRA, *Bunseki Kagaku* **33** (1984) T81.
8. M. ARITA, S. NASU and F. E. FUJITA, *Trans. Jpn Inst. Metals* **26** (1985) 710.
9. M. B. STEARNS, *Phys. Rev.* **129** (1963) 1136.
10. J. E. FRACKOWIAK, *Hyperf. Interact.* **28** (1986) 1067.
11. M. MIYAZAKI, M. ICHIKAWA, T. KOMATSU and K. NAKAJIMA, *J. Appl. Phys.* **69** (1991) 1556.
12. K. NOMURA, Y. UJIHIRA and H. YANAGITA, *Hyperf. Inter.* **88** (1994) 73.
13. L. DOBRZYNSKI, T. GIEBULTOWICZ, M. KOPCEWICZ, M. PIOTROWSKI and K. SZYMANSKI, *Phys. Status Solidi(a)* **101** (1987) 567.
14. K. ONO, Y. ISHIKAWA and A. ITO, *J. Phys. Soc. Jpn* **17** (1962) 1747.
15. J. E. FRACKOWIAK, *Hyperf. Interact.* **28** (1986) 1067.

Received 9 February 1993
and accepted 22 April 1994